Contents lists available at Science-Gate

International Journal of Advanced and Applied Sciences

Journal homepage: http://www.science-gate.com/IJAAS.html

Analysis of flow around high speed irregularly shaped bodies using numerical simulations

Alan Catovic *, Elvedin Kljuno, Avdo Voloder

Mechanical Engineering Faculty, University of Sarajevo, Sarajevo, Bosnia and Herzegovina

ARTICLE INFO

Article history:
Received 21 February 2018
Received in revised form
10 May 2018
Accepted 15 May 2018

Keywords:
Flow fields
Shock waves
Streamlines

ABSTRACT

Analysis of flow around the high-speed body with an irregular shape (such as fragments/shrapnels formed after the detonation of high explosive projectiles) was performed using the method of numerical simulations. For supersonic motion regime, pressure and velocity flow fields, as well as the formation of shock waves, around an irregularly shaped body were analyzed. Also, streamlines around an irregularly shaped body moving through the atmosphere were visualized (Ansys Fluent) and analyzed.

1. Introduction

Flows around irregularly shaped high-speed bodies are specific for viscous and compressible flow, dominant pressure force, shock waves, turbulent flow, unsteady flow fields, and most often by separating the boundary layer from the surface of the body during (Buresti, 2000).

Flows in which the Mach number is greater than 0.3 are considered compressible. Looking at the whole field simultaneously, four different speed regimes can be identified using Mach number as the criterion (Fig. 1): the *subsonic* flow (M <1 throughout the flow), the *transonic* flow (mixed regions where M <1 and M> 1), the *supersonic* flow (M> 1 in the entire flow) and the *hypersonic* flow (high supersonic velocities, M> 5) (Anderson, 2017).

The literature is somewhat deficient with analysis of flow around irregularly shaped bodies (specifically HE projectile fragments), using numerical simulation.

This paper is an attempt to give some light on phenomenology and the complexity of supersonic flow around such a body.

2. Shock waves

Shock waves are exceptionally thin regions across which the flow properties change drastically. In general, a shock wave will make an oblique angle with respect to the upstream flow. These are called oblique shock waves. A normal shock wave is simply a special case of the general family of oblique shocks, namely, the case where the wave angle is 90° In addition to oblique shock waves, where the pressure increases discontinuously across the wave, supersonic flows are also characterized by oblique expansion waves (Prandtl–Meyer waves), where the pressure decreases continuously across the wave. Oblique shock and expansion waves (Fig. 2) are prevalent in two- and threedimensional supersonic flows. The physical generation of waves in a supersonic flow—both shock and expansion waves—is due to the propagation of information via molecular collisions and due to the fact that such propagation cannot work its way into certain regions of the supersonic flow (Anderson, 2017).

Fig. 2 shows important parameters across oblique shock and expansion waves. Across the oblique shock wave, the Mach number discontinuously decreases, and the pressure, density, and temperature discontinuously increase. Across the expansion wave, the Mach number increases, and the pressure, temperature, and density decrease. Hence, an expansion wave is the direct antithesis of a shock wave.

The curved bow shock which stands in front of blunt bodies in a supersonic flow is shown in Fig. 3. Here, the shock wave stands a distance δ (shock detachment distance) in front of the nose of the blunt body. At point a, the shock wave is normal to the upstream flow, so the point a corresponds to a normal shock wave. Away from point a, the shock wave gradually becomes curved and weaker, eventually evolving into a Mach wave (pressure wave traveling with the speed of sound caused by a change of pressure in a compressible flow) at large

* Corresponding Author.
Email Address: catovic@mef.unsa.ba (A. Catovic)
https://doi.org/10.21833/ijaas.2018.08.001

distances from the body (illustrated by point e in Fig. 3).

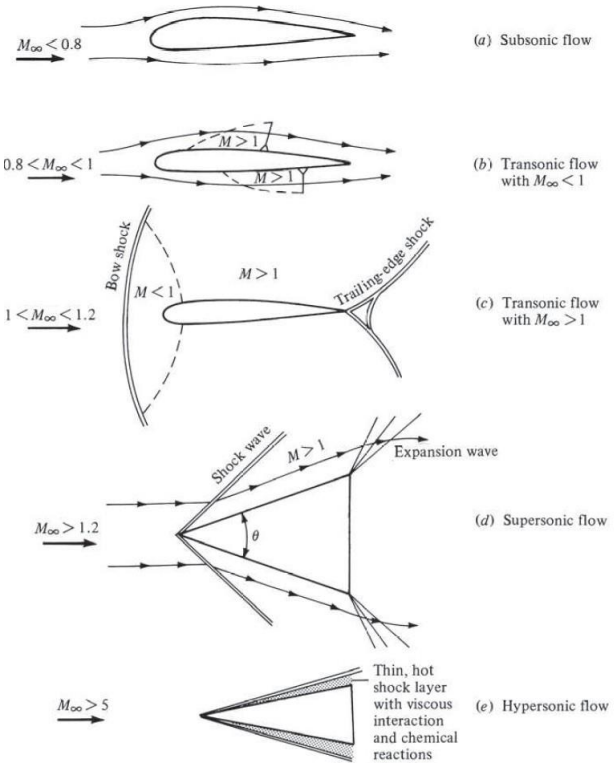

Fig. 1: Different regimes of flow (Anderson, 2017)

A curved bow shock wave is one of the instances in nature when one can observe all possible oblique shock solutions at once for a given freestream Mach number M_1. This takes place between points a and e (Fig. 3). Above the centerline, at point b, the shock is oblique. The flow is deflected slightly upward behind the shock at point b. As we move further along the shock, the wave angle becomes more oblique, and the flow deflection increases until the point c. Point c on the bow shock corresponds to the maximum deflection angle.

Slightly above point c, at point c', the flow behind the shock becomes sonic. From a to c', the flow is subsonic behind the bow shock; from c' to e, it is supersonic. Hence, the flow field between the curved bow shock and the blunt body is a mixed region of both subsonic and supersonic flow. The dividing line between the subsonic and supersonic regions is called the sonic line, shown as the dashed line in Fig. 3.

The shape of the detached shock wave, its detachment distance δ, and the complete flow field between the shock and the body depend on M_1 and the size and shape of the body. The solution of this flow field is not trivial. The supersonic blunt-body problem was a major focus for supersonic aerodynamicists during the 1950s and 1960s, spurred by the need to understand the high-speed flow over blunt-nosed missiles and reentry bodies. It was not until the late 1960s that sufficient numerical techniques became available for satisfactory engineering solutions of supersonic blunt-body flows (Anderson, 2017).

3. Numerical simulation method

The numerical simulations of the three-dimensional, compressible, turbulent, steady flow around the irregularly shaped body were performed in the Ansys Fluent CFD package for fragment in three different orientation. The basic equations of flow represent continuity equation, momentum equation and energy equation. The equation system is completed with the perfect gas equation of state and a thermodynamic state relation (Anderson, 2017).

The method of numerical simulations of air flow around an irregularly shaped body (fragment) consisted of: digitalization of the fragment model, physical domain discretization, characterization of materials, initial and boundary conditions, and solver and turbulence model selection.

The body was considered stationary (for a single orientation, Fig. 4) and the flow around it was analyzed. The velocity vector was directed in the positive direction of axes X, Y, and Z of the coordinate system set in the body center of mass (Fig. 4). The coordinate system in the initial position of the body coincides with the principal axes of inertia (defined in CAD and exported as iges format, together with the 3D body model).

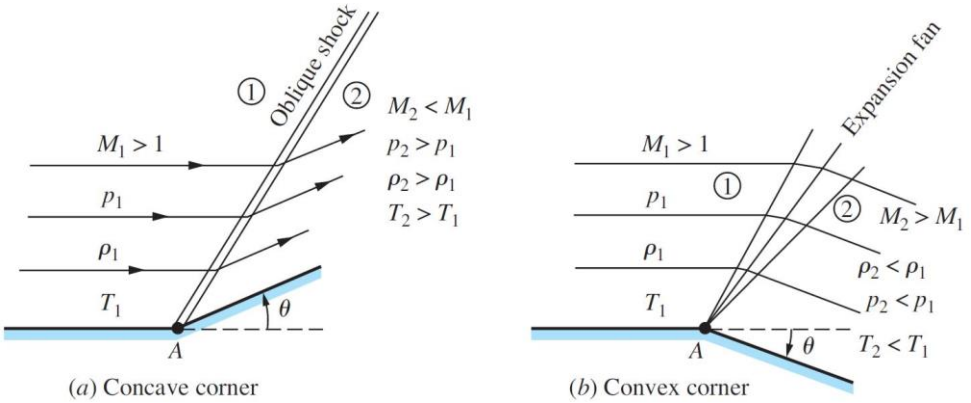

Fig. 2: Supersonic flow over a corner (Anderson, 2017)

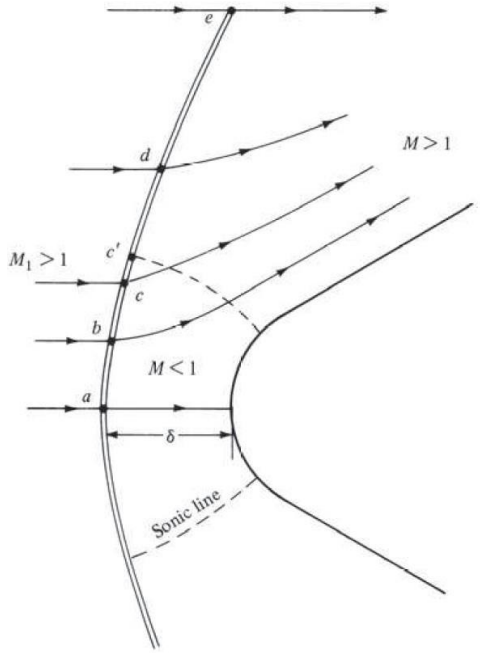

Fig. 3: Flow over a supersonic blunt body (Anderson, 2017)

Simulations of flow over the body for velocity of 3 Mach (velocity similar to an average initial velocity of HE projectile fragments) were carried out. In simulations, air is modeled as homogeneous, isotropic, ideal gas with pressure-temperature dependent density ρ, specific heat C_p, thermal conductivity k and dynamic viscosity μ. At the end of the domain, Pressure Farfield condition was used, which is commonly used in Fluent in aerodynamic simulations, where the effect of compressibility is dominant. The No Slip condition is defined on the surface of the body, which means that the relative flow velocity on the surface of the body is equal to zero. Boundary condition - the wall is used in the the case when the viscous effects cannot be ignored and is relevant to most fluid flow situations (Fluent, 2010). According to the recommendation (Fluent, 2010) for use with compressible flows, a density-based solver was selected in the simulations, where mass, flow, and energy equations are determined as the Navier-Stokes equation system in integral form for an arbitrary control volume.

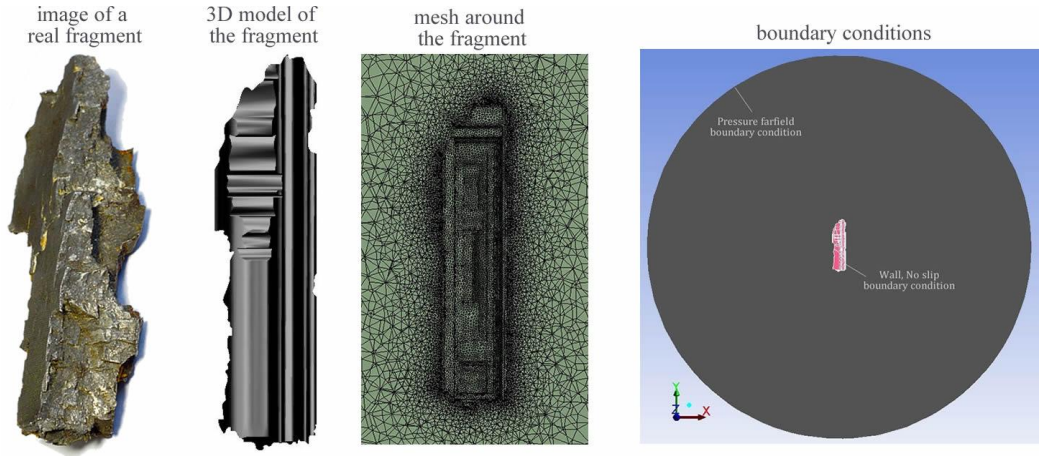

Fig. 4: Fragment shape, domain discretization and schematic of boundary conditions

According to the recommendations (Fluent, 2010), the Spalart-Allmaras turbulence model was used in the simulations. This model has been developed specifically for aerodynamic applications and has proven to be effective for the boundary layers with high-pressure gradients, and has been particularly effective for transonic flows around the aero profiles, including flows with significant separation of the boundary layer. The ever-increasing popularity of the Spalart-Allmaras model contributed to the rapid implementation of these models on unstructured meshes, unlike the classic aerodynamic turbulence models such as Baldwin-Lomax or Johnson-King (Pope, 2000; Rumsey, 2012).

4. Analysis of the results

Based on the results of the numerical simulations, an analysis of the pressure field, velocity field, streamlines and shock waves around the fragment was performed for three different orientations of the fragment, for an airflow velocity of 3 Ma.

The fluid resistance force it is the result of the action of normal force and tangential force on the body surface moving through the atmosphere. Main sources of the flow resistance to a moving body are practically three natural phenomena: fluid viscosity, shock waves (at speeds M ≥ 1), and turbulence behind the body.

The normal force (pressure force) is manifested in the pressure difference in front of the front of the body and behind the body. In the case of fragment, there is no clearly defined profile of the front and the back side since both sides involves complex and stochastic geometry of the fragment.

Tangential force is generated by friction (each fluid has viscosity) between fluid and body in the boundary layer. This resistive force depends primarily on the character of the flow in the boundary layer and the roughness of the body surface. The roughness affects not only the intensity

of the resistance but also the position of the point of transition of the laminar to the turbulent flow. In the case of a fragment, it is clear that we cannot talk about roughness, and certainly the irregular surface of the fragment further increases the tangential force because sharp edges lead to the creation of new shock waves and can cause separation of the flow and increase of the turbulence zone.

Fragment continually changes the value of its exposed surface during its motion (Kljuno and Catovic, 2017a), so at one point the fragment can represent a relatively slender body (fragment in the position with the minimum exposed area to the flow (Fig. 5), and at others it can represent blunt body (Fig. 5).

If the fragment starts to move from a relatively slender position (i.e., position represented in Fig. 5, last flow-field presented), the fragment boundary layer on the upper and lower surfaces experiences mild pressure gradients and there is no significant separation of the air flow. The turbulent flow behind the body is, in this case, smaller and the resistive force is predominantly due to viscous friction in the boundary layer.

However, by increasing the rotation angle of the body (Fig. 5), the pressure gradients increase considerably. The pressure gradient on the upper surface of the fragment then becomes so large that there is a separation of the flow which leads to the reduction of the pressure on the back side and the recirculation of the flow filled with the vortices that dissipate part of the mechanical energy (mainly in the form of heat) and thus increase the total drag force. Vortices are usually in mutual interaction; they are movable and can exchange energy. That is why pressure drag increases, and when the fragment is exposed to fluid flow through its larger surface (practically represent a blunt body), the pressure drag is then much higher than the friction drag.

Pressure and velocity fields, shown in Figs. 5 and 6, are complex and asymmetrical because the fragment is an irregularly shaped body with a large number of bumps, edges and dents, and it is known that the character of flow field is mostly dependent on the shape of the body (as well as flow velocities and fluid characteristics).

As expected for the supersonic flow, there is significant overpressure zone in front of a fragment, while behind a fragment there is a region of underpressure, which leads to increase in drag force.

In the case where the velocity vector is perpendicular to the maximum exposed area of the fragment (Fig. 5) - the overpressure zone in front of the fragment is the largest (widest) and the smallest in the case where the velocity vector is perpendicular to the minimum exposed fragment area (Fig. 5). Similarly applies to the region of underpressure.

As far as velocity fields are concerned, in the case when the velocity vector is perpendicular to the largest exposed area of the fragment (fragment can be considered as a blunt body, Fig. 6), the greatest decrease of the flow velocity is reached; in case of minimum exposed fragment area (fragment can be considered as a slender body, Fig. 6) one can notice more moderate reduction in the flow velocity with the least pronounced zone in which this velocity reduction occurs.

Of the greatest significance for the movement of the fragment itself through the atmosphere as a resistive medium are certainly the shock waves occurring at the supersonic flow. Since the flow velocity was 3 Mach in our case, this implies the appearance of the shock waves around the fragment. The fragment is irregularly shaped, with a large number of edges and curved surfaces, which results in the creation of a larger number of shock waves along the fragment (best seen in Figs. 5 and 6).

It is known that significant compressibility effects are present in supersonic flows. For the same flow velocity (of an irregularly shaped rotating body), the body will have the shock waves more stretched towards the body in the position with the smaller exposed area of fragment perpendicular to velocity vector (Fig. 5). In Fig. 5 there is a noticeable irregularity of the fragment shape which causes the formation of a number of smaller shock waves along its surface (the fragment has quite a number of sharp edges that cause the emergence of new oblique shock waves). The appearance of these side shock waves leads to a local increase in the drag force.

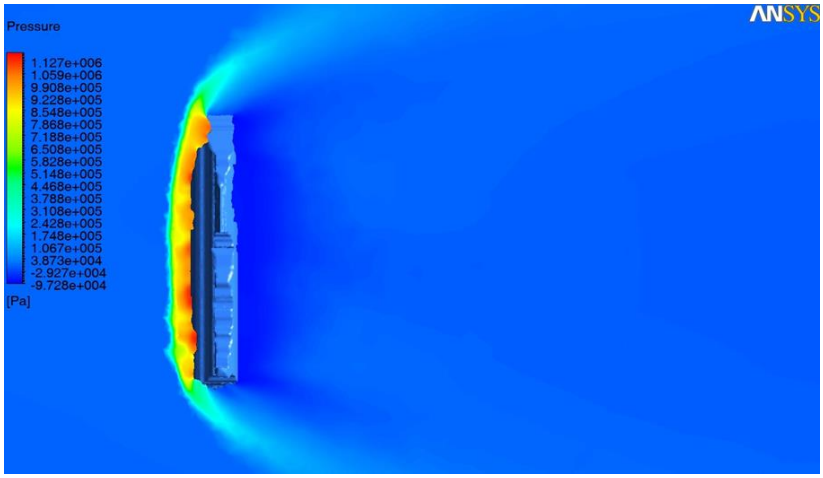

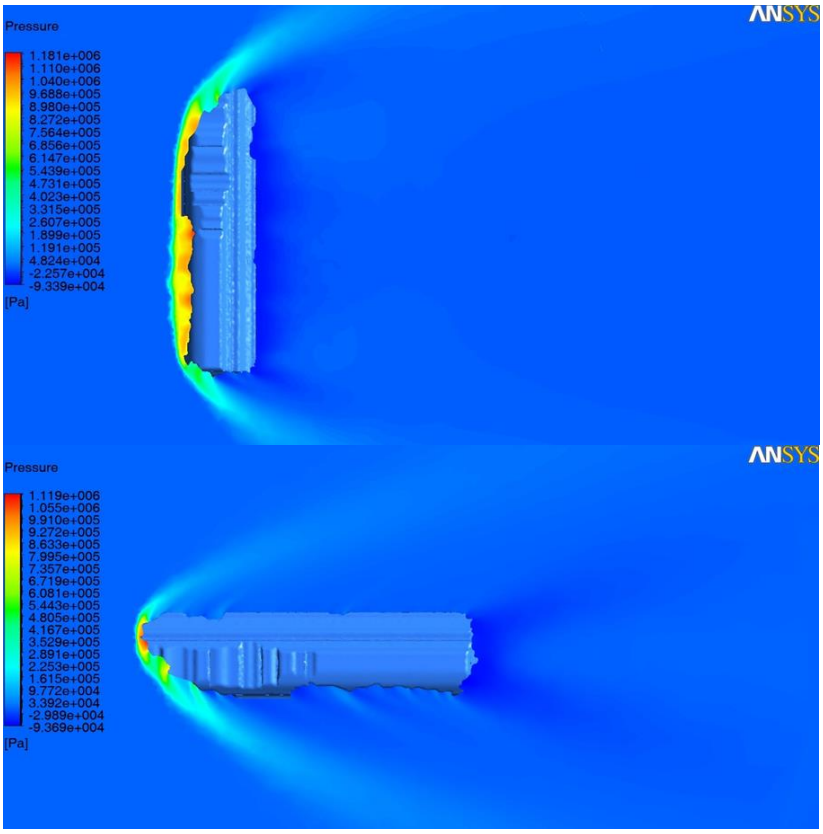

Fig. 5: Pressure field around fragment (in a plane crossing its center of mass) for 3 different orientation of fragment, for air flow velocity of 3 Mach

Fragmentation of HE projectile creates thousands of fragments that are moving through the air. In the initial phase of movement, these fragments are relatively close to each other, which can lead to the interaction of the shock waves around individual fragments and the introduction of additional instability in their movement. In addition, fragments are usually unstable, (Kljuno and Catovic, 2017b) which further complicates the whole process and destabilizes the fragments. In available literature, this is often not mentioned.

Generally speaking, the supersonic flow regime around all bodies is characterized by pronounced shock waves (Figs. 5 and 6), extremely narrow fluid regions where the flow characteristics change discontinuously in a very short time interval, with the pressure gradients being exceptionally large. In front of the shock wave, there is a zone of undisturbed flow, while behind it there is a zone in which there are large differences in pressure, velocity, temperature, and density.

The fluid layer between the shock waves and the body (called the shock layer) is particularly important in the case of blunt bodies (such as HE projectile fragments,) when curved bow shock waves occur (Figs. 3, 5, and 6). For the shock layer, except high pressure, high temperatures and high flow densities are also characteristic.

The characteristic oblique and expansion shock waves around the fragment can best be seen in Fig. 5. Oblique shock waves are located in front and laterally of the fragment, and the expansion shock waves on the back side of the fragment. There are several oblique shock waves observed along the fragment at points where the geometry of the fragment (pronounced edges on fragment surface) changes.

In the case when flow velocity vector was perpendicular to minimum exposed area of fragment (Fig. 5), oblique shock wave angle is smaller and wave envelops the fragment more tightly. Also, it is known that when flow velocity increases, oblique shock waves are closer to the body, which means that ie the shock waves at M = 4 will be closer to the body than at the velocities of M = 2.

In the case when flow velocity vector was perpendicular to the maximum exposed area of the fragment (Fig. 5) a bow shock wave occurs. The bow shock wave (schematically shown at 3) appears in supersonic fluid flow around the blunt body when the angle of the tip of the body is larger than the critical angle - at which the separation of the waves begins (Fig. 3). From the theory of shock waves (Anderson, 2017), this angle, theoretically, at $M = \infty$ and $\gamma = 1.4$ has the highest possible value $\theta = 45{,}5°$, after which the shock wave separates from the top of the body.

In Fig. 5 above, between the bows shock wave in front of the fragment and the fragment itself, there is a mixed flow zone where there is a subsonic and supersonic flow. The streamlines around the fragment (Fig. 7) also confirm this mixing, where the flow vortex that increases the drag force can be seen in front of the fragment.

It is important to note that the bow shock waves significantly increase the drag force of supersonic

bodies, which is utilized ie in the design of space capsule (Apollo program) that require a high degree of drag to prevent the capsule from burning upon reentering the atmosphere (Anderson, 2017). In the case of a fragment, the presence of a bow shock wave also leads to an increase in the drag force.

In Fig. 6 the streamlines around the fragment are presented for three different orientation of fragment (relative to the flow velocity vector), and for a flow velocity of 3 Mach. A streamline is a path traced out by a massless particle as it moves with the flow. Streamlines are a family of curves that are instantaneously tangent to the velocity vector of the flow.

The most intensive recirculation and partial separation of the flow occur in the case when flow velocity vector is perpendicular to the largest exposed area of the fragment (Fig. 6), which is more clearly visible in Fig. 7 (zoomed display of streamlines around the fragment with maximum exposed area perpendicular to velocity vector).

Interestingly, the bottom (end) area of this particular fragment is coincidentally somewhat streamlined (bottom part of the fragment gradually narrows, as shown Fig. 6 in the middle), so there is no significant separation of the flow for this case. For the same fragment, the front side is blunt, so a recirculation of the flow also occurs.

In the case of flow around fragment in blunt position (flow perpendicular to maximum exposed area of fragment, presented in Fig. 7), there are several recirculation zones, each of which is irregular, asymmetric and stochastic. In this case, there is also a recirculation area of the flow in front of the fragment itself, which is quite interesting and one does not often come across this phenomena in engineering problems.

These zones occur at points where fragment geometry changes (especially on concave parts of the front surface of the fragment) and can increase the total drag force.

Relative motion of fluid from the region of high pressure to the region of low pressure, combined with fluid movement in the direction of flow, leads to the formation of a vortex flow behind the fragment, dissipating the energy, thereby significantly increasing the drag force.

In the case of flow around fragment in a position where its minimum exposed area is perpendicular to flow velocity vector (Fig. 5 and Fig. 8), partial flow separation is practically present only in the zone behind the fragment. In this zone, recirculation of the flow is also noted, but in a much smaller extent than in the case when the maximum exposed area of the fragment (Fig. 8) is perpendicular to the velocity vector. Because of this, the drag force in this case is much smaller.

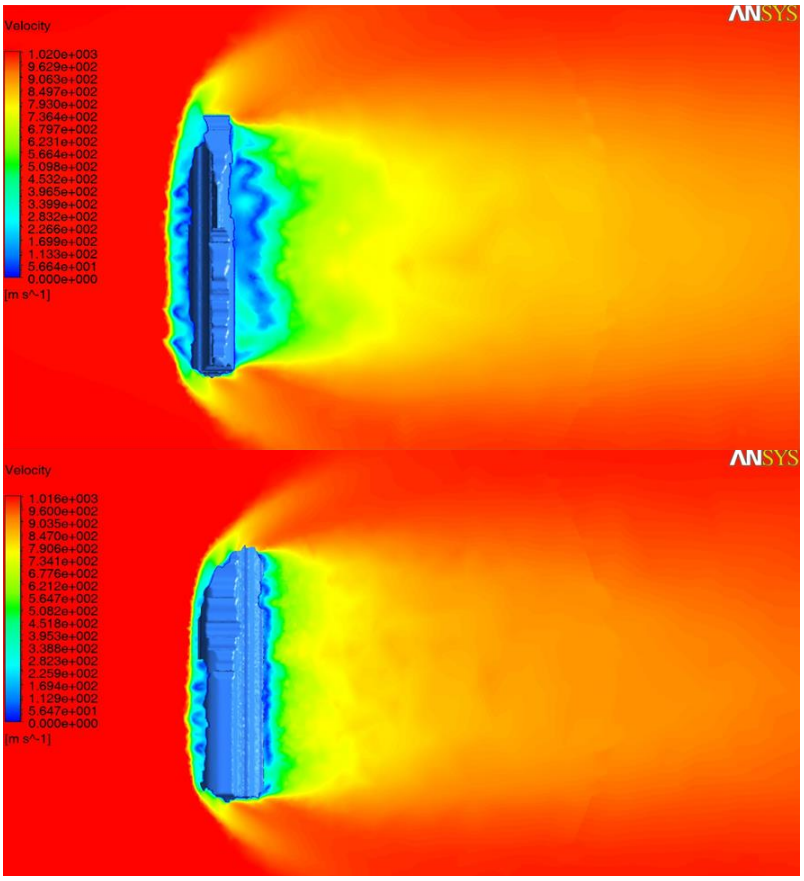

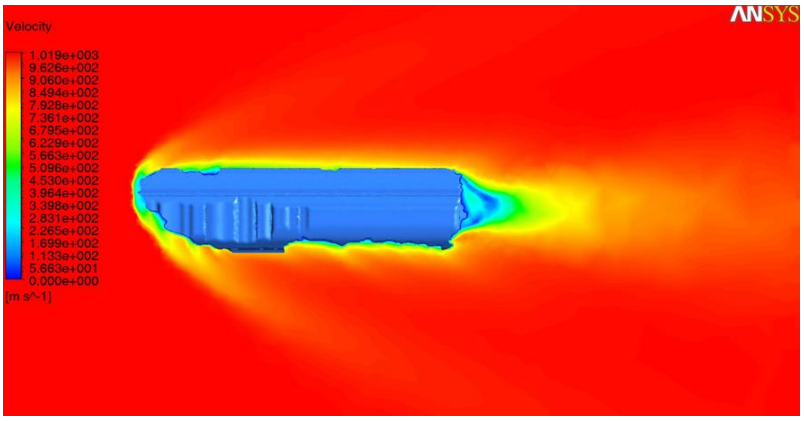

Fig. 6: Velocity field around fragment (in a plane crossing its center of mass) for 3 different orientation of fragment, for air flow velocity of 3 Mach

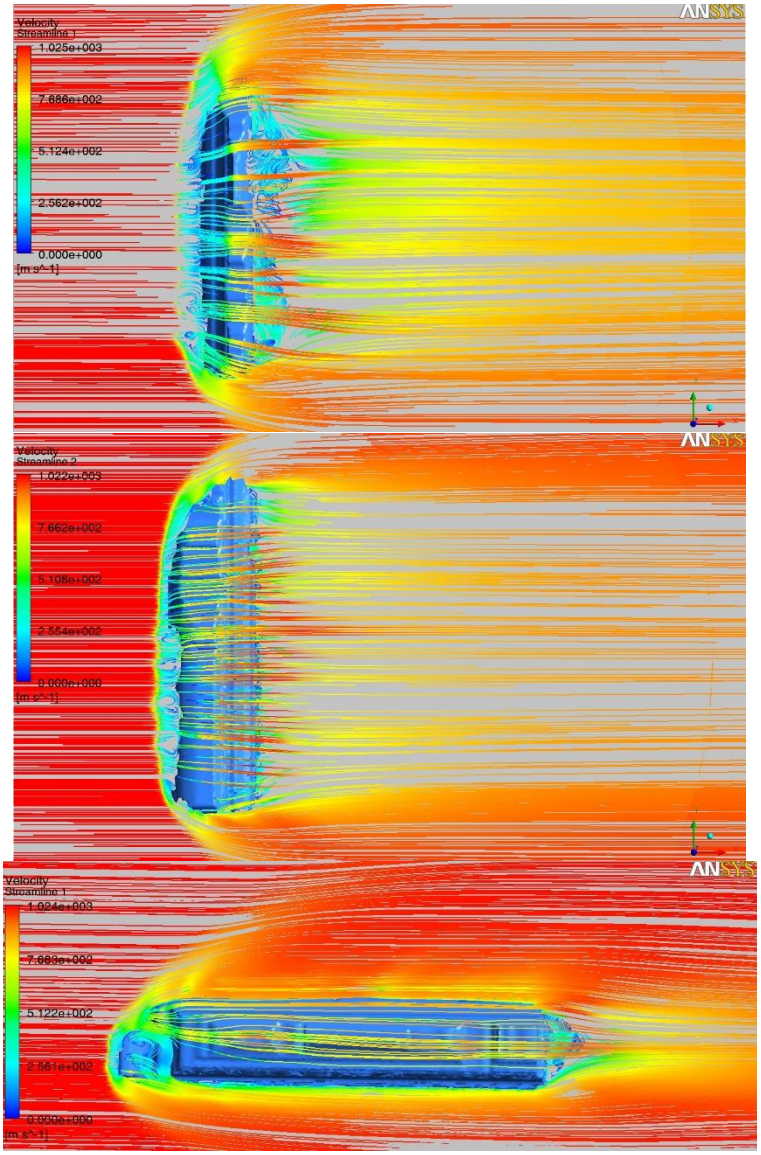

Fig. 7: Streamlines around fragment for 3 different orientation and for flow velocity 3 Mach

Figs. 8 and 9 show zoomed-in representation of the streamlines around fragment, for the case when the maximum exposed area of the fragment (Fig. 8) is perpendicular to the velocity vector and when the minimum exposed area of the fragment is perpendicular to the flow velocity vector (Fig. 9). Flow velocity was also 3 Mach (~ 1020 m/s).

Fig. 10 shows the pressure field flow around fragment in three different planes (a plane through the center of fragment's mass (Fig. 10), plane 3mm in front of the center of mass (Fig. 10), plane 3mm behind the center of mass (Fig. 10).

Since the shape of the fragment is irregular, an overpressure zone (and the underpressure zone) is not symmetrical for different planes of fluid flow and

varies considerably both in appearance (zone width) and quantitatively (different values of p and v). This can be clearly visible in Fig. 10.

The shape of the shock waves around the fragment is not the same and they are not symmetrical because the fragment is irregular and for different flow planes around the fragment, shock waves have a slightly different shape (Fig. 10).

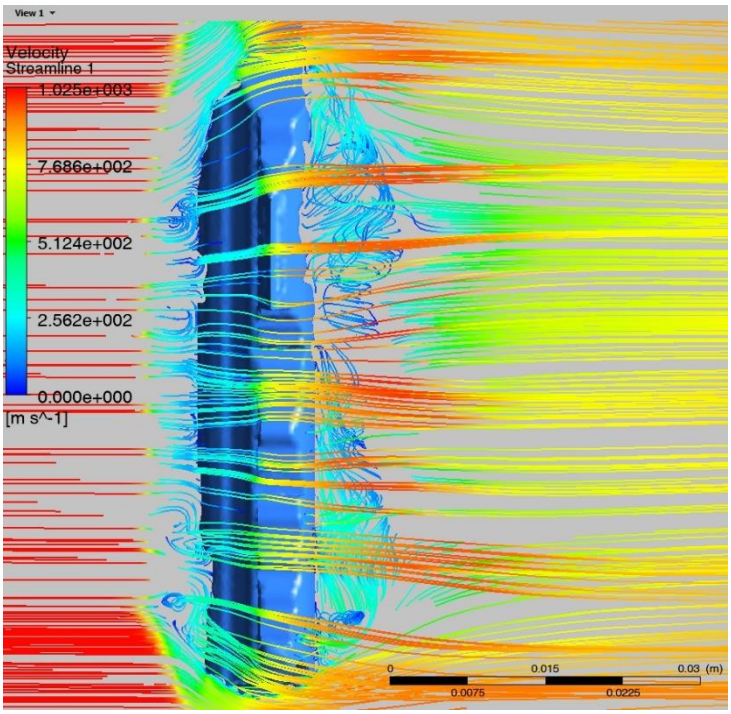

Fig. 8: Zoomed display of streamlines around the fragment with maximum exposed area perpendicular to velocity vector (flow velocity 3 Mach)

On the other hand, in Fig. 11, the pressure field at 3 Ma on the fragment itself is shown in two different projections. Fig. 11, which shows the pressure field on the fragment in two different projections, clearly shows an unequal (asymmetrical) distribution of pressure around fragment. Here, it is interesting to note that in front of the fragment, when the larger exposed area of the fragment is perpendicular to velocity vector (Fig. 5), local pressure increases in certain parts of the flow.

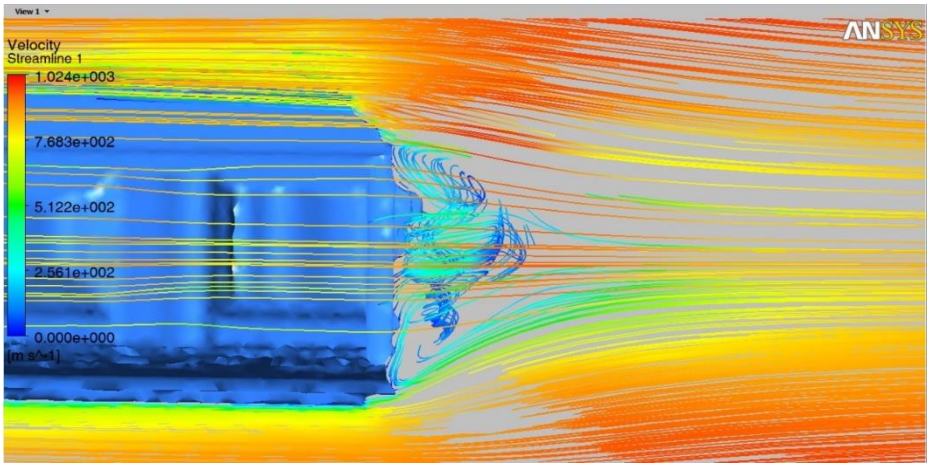

Fig. 9: Zoomed display of streamlines around back side of the fragment with minimum exposed area perpendicular to velocity vector (flow velocity 3 Mach)

These "mini" zones are more clearly seen on the diagrams of pressure field (Fig. 5 and Fig. 11).

The fragment is irregularly shaped and the fluid flow, even in front of the fragment (for the position of the fragment in which it can be considered a blunt body), is curled in certain parts of the flow (in the "pockets" of the front surface of the fragment, see Fig. 11).

The analysis of the pressure field, velocity field, and streamlines around the fragment (irregularly shaped bodies) shown in this paper, as can be clearly seen, gives us an insight into the complexity of the problem of moving of real fragments through the atmosphere (such as motion of primary and secondary fragments formed after the explosions). It is practically impossible to adequately investigate

these problems without using numerical simulations as one of the methods of research.

Also, every fragment has different (irregular, stochastic) shape, and this further complicates matter during the research.

This kind of research can also be used in conjunction when predicting the motion of fragment, where it is already established (Kljuno and Catovic, 2017c) that the trajectory of the fragment is strongly influenced by the lateral component of the aerodynamic force - which leads to the significant sideways motion of the body (because the flow field around fragment is not symmetrical).

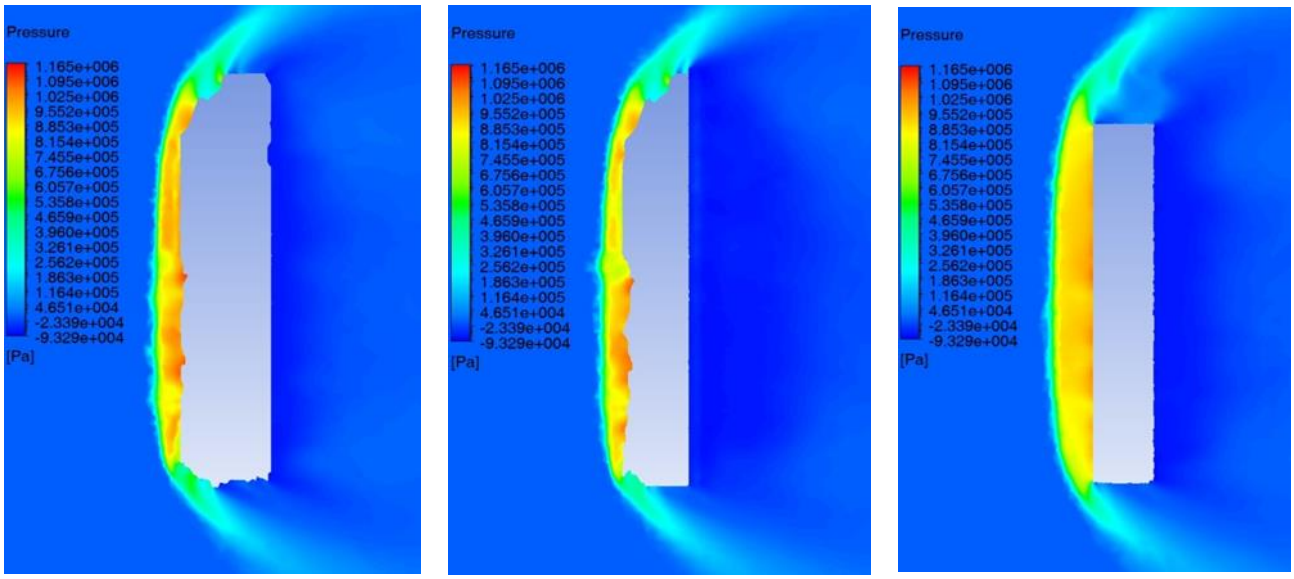

Fig. 10: Pressure field flow around fragment in three planes (plane through the center of mass (left), plane 3mm in front of the center of mass (middle), plane 3mm behind the center of mass (right))

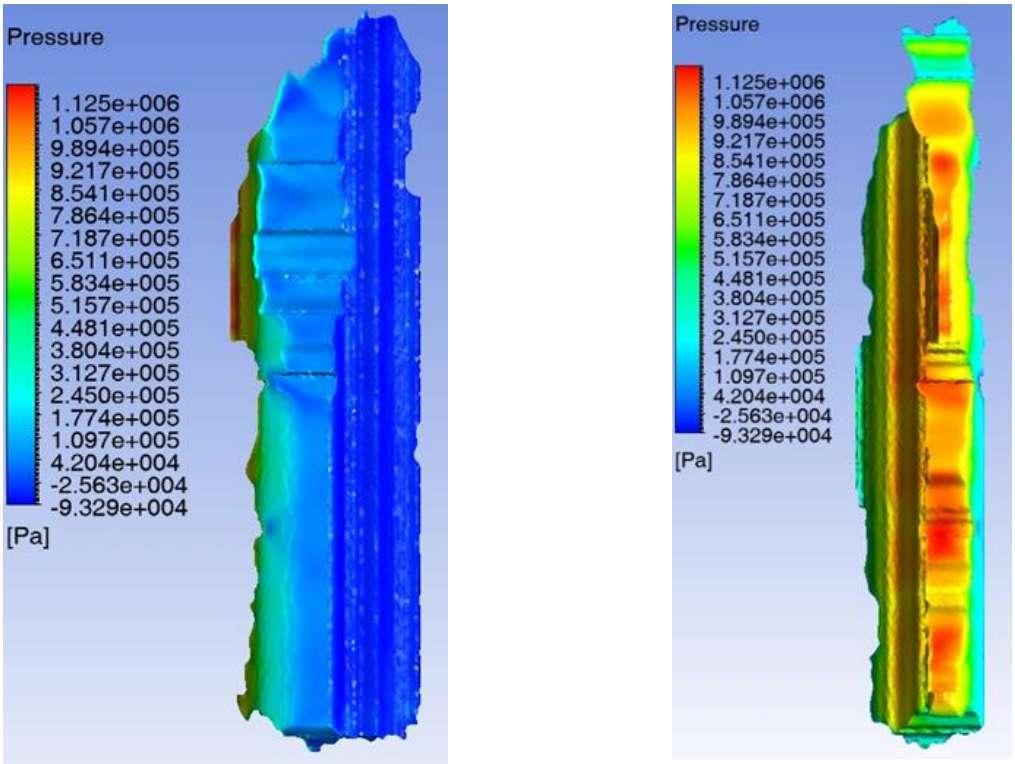

Fig. 11: Pressure field (at 3 Ma) on the fragment itself, shown in two different projections

5. Conclusion

An analysis of the pressure field, velocity field, streamlines and shock waves around the fragment was performed for three different orientations of the fragment, for an airflow velocity of 3 Ma.

Pressure and velocity fields are complex and asymmetrical because the fragment is an irregularly shaped body with a large number of bumps, edges and dents.

There is significant overpressure zone in front of a fragment, while behind a fragment there is a region of underpressure, which leads to increase in drag force.

The fragment is irregularly shaped, with a large number of edges and curved surfaces, which results

in the creation of a larger number of shock waves along the fragment. Oblique shock waves are located in front and laterally of the fragment, and the expansion shock waves on the back side of the fragment. Between the bow shock wave in front of the fragment and the fragment itself, there is a mixed flow zone where there is a subsonic and supersonic flow.

The most intensive recirculation and partial separation of the flow occur in the case when flow velocity vector is perpendicular to the largest exposed area of the fragment

Since the shape of the fragment is irregular, an overpressure (and an underpressure) zone is not symmetrical for different planes of fluid flow and varies considerably both in appearance (zone width) and quantitatively (different values of p and v).

The fragment is irregularly shaped and the fluid flow, even in front of the fragment (for the position of the fragment in which it can be considered a blunt body), is curled in certain parts of the flow (in the "pockets" of the front surface of the fragment).

Follow up research should deal with the analysis of the mutual interaction of shock waves of several fragments moving together through the air

References

Anderson JD (2017). Fundamentals of Aerodynamics. 6th Edition, McGraw-Hill Editions, New York, USA.

Buresti G (2000). Bluff-body aerodynamics lecture notes. Department of Aerospace Engineering, University of Pisa, Italy.

Fluent A (2010). Ansys fluent theory guide, Version 13.0. Ansys Inc., Canonsburg, USA.

Kljuno E and Catovic A (2017a). Instability estimation of irregularly shaped bodies moving through a resistive medium with high velocity. International Journal of Advanced and Applied Sciences, 4(9): 70-79.

Kljuno E and Catovic A (2017b). Determination of the center of pressure and dynamic stability for irregularly shaped bodies. International Journal of Advanced and Applied Sciences, 4(10): 1-9.

Kljuno E and Catovic A (2017c). Prediction of the trajectory of an irregularly shaped body moving through a resistive medium with high velocities. International Journal of Advanced and Applied Sciences, 4(11): 1-10.

Pope SB (2000). Turbulent Flows. Cambridge University Press, Cambridge, UK.

Rumsey C (2012). Turbulence modeling. NASA Langley Research Center, Hampton, USA.